Investigation of the energy dependence of the spin-spin correlation in the diproton-resonance region

N. S. Borisov, V. G. Vovchenko, V. A. Efimovykh, A. A. Zhdanov, M. Yu. Kazarinov, Yu. M. Kazarinov, Yu. F. Kiselev, A. I. Kovalev, M. Yu. Liburg, B. S. Neganov, V. V. Polyakov, V. E. Popov, A. N. Prokof'ev, V. Yu. Trautman, Yu. A. Usov, and A. V. Shvedchikov

Leningrad Institute of Nuclear Physics, Academy of Sciences of the USSR

The polarization correlation coefficient C_{NN} in pp scattering has been measured at nine incident-proton energies in the range 550–950 MeV. Structure is found in the energy distribution of $C_{NN}(90°)$, the distribution having a maximum at $T \approx 700$ MeV. The data are compared with the predictions of Hoshizaki's phase-shift analysis and it is shown that the results of the analysis do not agree with the experimental results. The behavior of the matrix elements of the scattering amplitude at $\Theta = 90°$ is discussed; the behavior of the matrix elements clearly confirms resonance pp interaction only in the $^1D_2$ state.

PACS numbers: 13.75.Cs

I. INTRODUCTION

The discovery of structure in the energy dependence of the cross sections for elastic scattering of protons by protons in pure spin states has led to the appearance of papers on the spin dependence of the nucleon-nucleon interaction at intermediate energies. Measurements of the difference $\Delta\sigma$ between the total interaction cross sections for longitudinally polarized protons[1] ($\Delta\sigma_L = \sigma_{\rightrightarrows} - \sigma_{\rightleftarrows}$) and transversely polarized protons[2] ($\Delta\sigma_T = \sigma_{\uparrow\downarrow} - \sigma_{\uparrow\uparrow}$) revealed features that might be explained under the assumption that the interaction between two protons is of resonance type.[3] A phase-shift analysis of the data in the region 0.5–2 TeV in which the results of Refs. 1 and 2 were taken into account indicated that the hypothesis of resonance in pp scattering is consistent with the experimental data.[4] Although such an analysis is quite crude, it still made it possible to estimate the expected energy and angular dependences of the observed quantities and to select the measurements that would most clearly reveal the effects of a resonance interaction. Those measurements include measurements of the components of the polarization-correlation, depolarization, and polarization-transfer tensors.

The current status of the diproton-resonance problem is reflected in Table I.

Theoretical analysis of the problem[6,7] is not convincing enough, so experimental research still remains the principal method of solving it.

In particular, measurements of the components of the polarization correlation tensor may provide important information for the solution of the problem of dibaryon resonances. This is connected with the possibility of clarifying the relations between the contributions from the triplet and singlet interactions. The problem is considerably simpler for the c.m. angle $\theta = 90°$, since then it is sufficient to measure only the coefficient C_{NN} (where N is the normal to the scattering plane) and the differential scattering cross section in order to extract the singlet part of the pp interaction:

$$\frac{d\sigma_0}{d\Omega}(90°) = \frac{1}{4}|M_{ss}|^2 + \frac{1}{2}|M_{01}|^2 + \frac{1}{2}|M_{10}|^2, \tag{1}$$

$$\frac{d\sigma_0}{d\Omega}(90°)\,[1 - C_{NN}(90°)] = \frac{1}{2}|M_{ss}|^2, \tag{2}$$

where $d\sigma_0/d\Omega$ is the differential cross section for elastic scattering of unpolarized protons by an unpolarized target, while M_{ss}, and M_{01} and M_{10} are the singlet and triplet elements of the scattering matrix, respectively. The equation

$$C_{NN}(90°) = \frac{d\sigma_t/d\Omega - d\sigma_s/d\Omega}{d\sigma_0/d\Omega}\bigg|_{\theta=90°}, \tag{3}$$

in which $d\sigma_t/d\Omega$ and $d\sigma_s/d\Omega$ are the differential cross sections for elastic scattering in the triplet and singlet states, follows immediately from Eqs. (1) and (2). Even the sign of C_{NN} shows which type of interaction is dominant. In some cases a more detailed analysis of the energy and angular dependences of C_{NN} makes it possible to distinguish the contributions to the scattering process from individual states. Additional information can be obtained by measuring the correlation coefficient C_{LL} for scattering of a longitudinally polarized beam by a longitudinally polarized target:

$$\frac{d\sigma_0}{d\Omega}(90°)C_{LL}(90°) = -\frac{1}{4}|M_{ss}|^2 - \frac{1}{2}|M_{10}|^2 + \frac{1}{2}|M_{01}|^2. \tag{4}$$

Measurements of $d\sigma_0/d\Omega$, C_{NN}, and C_{LL} at $\theta = 90°$, taken together, make it possible to distinguish the contributions from the individual matrix elements that determine the scattering at that angle.

Measurements of the coefficient $C_{NN}(\theta)$ at 550, 610, and 630 MeV have been made[8] at the JINR synchrocyclotron. When the present work was begun there were virtually no data on C_{NN} at energies E above 630 MeV, since the measurements reported in Ref. 9 at

TABLE I. Proposed resonance states of the two-proton system (Ref. 5).

Resonance	Mass, GeV	Width, MeV	State
B_1^2 (2.14)	2.14–2.17	50–100	$^1D_2$
B_1^2 (2.18)	2.18–2.22	100–200	$^3P_{0,1,2}$
B_1^2 (2.22)	2.20–2.26	100–200	$^3F_3$
B_1^2 (2.43)	2.43–2.50	150	$^1G_4$

683, 735, and 978 MeV were not accurate enough to permit any definite conclusions to be drawn concerning the trend of C_{NN} as a function of θ and E. We accordingly measured C_{NN} at $\theta = 50°$ and $90°$ in the energy interval 690–950 MeV. The purpose of the experiment was to obtain data on the behavior of the polarization correlation coefficient C_{NN} in the region of the proposed dibaryon resonances with the accuracy that can be achieved with present-day polarized proton targets. The measurements of the polarization in pp scattering at $\theta = 50°$ made it possible to compare the values obtained with the known value of $\langle P(50°)\rangle$ and thereby to test the reliability of the measurements.

Measurements of C_{NN} at energies below 580 MeV have been made again[10] at SIN, and such measurements at higher energies have been carried through by two groups[11] in the USA. A joint analysis of all the data on the energy dependence of the correlation coefficients $C_{NN}(90°)$ and $C_{LL}(90°)$ in the range 0.5–1.5 GeV makes it possible to draw definite qualitative conclusions concerning the parts played by different spin states in the pp elastic scattering process.

II. EXPERIMENTAL SETUP

When a proton beam of polarization P_B is scattered by a target of polarization P_T, the intensity $I(\theta)$ of the protons scattered at the angle θ in the c.m.s. is given by

$$I(\theta) = I_0(\theta) [1 + (P_B + P_T)P + C_{NN}P_B P_T],\qquad(5)$$

where $I_0(\theta)$ is the intensity for scattering of an unpolarized beam by an unpolarized target and P is the polarization in pp scattering. The vectors P_B and P_T are perpendicular to the scattering plane. For scattering at $\theta = 90°$ we have

$$I(90°) = I_0(90°) [1 + C_{NN}P_B P_T].\qquad(5a)$$

By changing the directions of the beam and target polarizations one can measure four intensities I_{++}, I_{--}, I_{+-}, and I_{-+}, which differ in the sign of the beam polarization (first subscript) or the target polarization (second subscript). Because the beam protons are scattered both by free protons and by nucleons bound in nuclei occurring in the structure of the polarized target, the liquid helium, and the mechanical parts of the target, the measured intensities I_{ik} should be expressed as follows:

$$I_{++}(\theta) = I_0(\theta) [1 + (P_B + P_T)P + C_{NN}P_B P_T] + I_{+b},$$
$$I_{+-}(\theta) = I_0(\theta) [1 + (P_B - P_T)P - C_{NN}P_B P_T] + I_{+b},$$
$$I_{-+}(\theta) = I_0(\theta) [1 - (P_B - P_T)P - C_{NN}P_B P_T] + I_{-b},\qquad(6)$$
$$I_{--}(\theta) = I_0(\theta) [1 - (P_B + P_T)P + C_{NN}P_B P_T] + I_{-b},$$

where the subscript b refers to background measurements.

The coefficients $C_{NN}(\theta)$ and polarizations $P(\theta)$ are determined from Eqs. (6) as follows:

$$C_{NN}(\theta) = \frac{1}{P_B P_T} \frac{(I_{++} + I_{--}) - (I_{+-} + I_{-+})}{\sum I_{ik} - 2(I_{+b} + I_{-b})},\qquad(7)$$

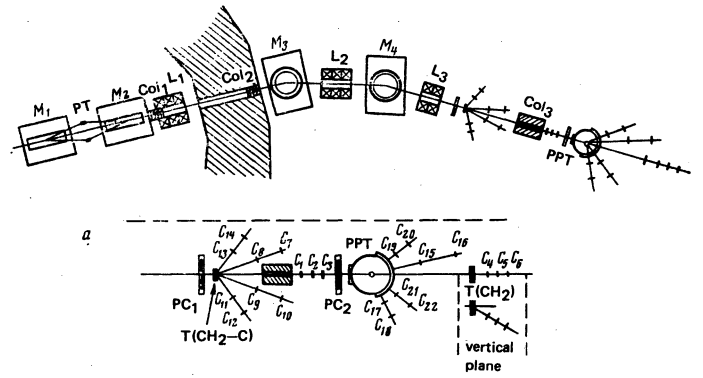$$P(\theta) = \frac{1}{P_T} \frac{(I_{++} + I_{-+}) - (I_{--} + I_{+-})}{\sum I_{ik} - 2(I_{+b} + I_{-b})},\qquad(8)$$

FIG. 1. Experimental setup: PT—polarizing target, M_1–M_4—magnets, L_1–L_3—quadrupole lenses, Col_1–Col_3—collimators, PPT—polarized proton target, PC_1–PC_2—proportional chambers, C_1–C_{22}—scintillation counters, $T(CH_2)$ and $T(CH_2–C)$—monitor and polarimeter targets.

$$P(\theta) = \frac{1}{P_B + P_T} \frac{2[(I_{++} - I_{+b}) - (I_{--} - I_{-b})]}{\sum I_{ik} - 2(I_{+b} - I_{-b})},\qquad(9)$$

where

$$\sum_a I_{ik} = I_{++} + I_{--} + I_{+-} + I_{-+}.$$

Since the measured quantities enter in Eqs. (7) and (8) in virtually the same way, the errors in the measurements of the intensities I_{ik} and the background should have similar effects on the values of C_{NN} and P. The determination of the latter from the four measured intensities minimizes the errors due to instability of the apparatus and to spurious asymmetries.

1. General setup of the experiment

The general setup of the experiment at 690–950 MeV is shown in Fig. 1. This setup differs from that used in the earlier measurements at 550–630 MeV in that the position of the polarized beam is more strictly monitored. The proton beam extracted from the synchrocyclotron is deflected by the magnet M_1 onto the 10-cm thick beryllium polarizing target (PT). The magnet M_2 returns the protons scattered through the angle $(7.5 \pm 0.2)°$ to their initial direction. The polarization of the scattered beam (see Table II) amounted to $\approx 30\%$. The magnets M_3 and M_4 cleared the polarized-proton beam, improved the momentum resolution of the channel, and were used to direct the beam accurately onto the center of the polarized target. The beam was shaped by a system of quadrupole lenses (L_1, L_2, L_3) and collimators (Col_1, Col_2, Col_3). By changing the polarity of the magnets M_1 and M_2 and the position of the polarizing target

TABLE II. Characteristics of the polarized proton beams.

Energy, MeV	Intensity on the target, sec^{-1}	Polarization	$\langle P(45°)\rangle$
690±30	2.4·10^5 } *	0.284±0.006	0.514±0.008
760±30	7.6·10^5	0.291±0.007	0.508±0.008
804±23	6.8·10^5	0.289±0.006	0.482±0.008
892±20	1.3·10^6 } **	0.300±0.008	0.430±0.008
950±17	9.0·10^6	0.300±0.008	0.419±0.008

*On a 9-cm^2 area; **on a 4-cm^2 area.

we could reverse the direction of the beam polarization without altering its magnitude. The protons scattered to the left by the polarizing target were preferentially oriented spin up (positive polarization, the L beam), while those scattered to the right were oriented spin down (negative polarization, the R beam). The absolute value of the beam polarization P_B varied from run to run by no more than 0.01; the variations were mainly due to inaccurate setting of the angle of the polarizing scattering. When the sign of the polarization was changed, its magnitude remained the same within the accuracy of the measurements, i.e., within 0.5%.[12]

The momentum resolution for 950-MeV protons was $\Delta p/p = \pm 0.012$. Paraffin absorbers mounted in front of the collimator Col_2 were used to alter the beam energy. This caused the momentum resolution of the channel to deteriorate because of multiple scattering of beam particles and straggling. The momentum scale of the channel was calibrated by the current carrying filament method. The multiwire proportional chambers PC_1 and PC_2 and the scintillation counters C_1-C_3 (Fig. 1, a) were used to locate the beam and then to monitor the spatial and angular distributions of the beam particles. On reversing the beam polarization, the position of the center of gravity of the intensity distribution of the beam on the target and the angular spread of the beam did not change by more than ± 1 mm and $\pm 0.03°$, respectively. The spatial and angular distributions of the protons in the L and R beams also remained the same after the beam passed through the absorber and lost energy.

The polarization of the beam was measured with a two-arm polarimeter comprising the scintillation counters C_7-C_{14}. We recorded pp scattering events to the left and right at angles corresponding to $45°$ in the c.m.s. for each energy. Targets of CH_2 and carbon (C), each having the same stopping power, were used as polarimeter targets. The beam polarization was determined from the observed asymmetry and the known polarization in pp scattering:

$$P_B = \langle \varepsilon \rangle / \langle P(45°) \rangle. \tag{10}$$

The value of $\langle \varepsilon \rangle$ was obtained by averaging the asymmetries for the L and R beams:

$$\langle \varepsilon \rangle = \frac{\varepsilon_L + \varepsilon_R}{2}, \quad \varepsilon_{L,R} = \left(\frac{l-r}{l+r} \right)_{L,R} \tag{11}$$

(l and r are the numbers of counts for the left- and right-hand channels, respectively). The value of the polarization $\langle P(45°) \rangle$ was determined for each energy by approximating all the known experimental data on the angular dependence of the polarization in the energy range 0.5–1.2 GeV.[13] The asymmetries ε_L and ε_R were measured at least three times for each energy with a statistical error smaller than 2.5×10^{-3}. The difference between the values of $\langle \varepsilon \rangle$ for different runs never exceeded twice the statistical error; this indicates the stability of the operation of the polarized-beam transport system. The uncertainty $\Delta \varepsilon$ in the asymmetry due to differences in the spatial and angular distributions of the L and R beams also never exceeded 2×10^{-3}, i.e. it was smaller than the statistical error.

The absolute value of the error in determining the

beam polarization, including the statistical error in measuring $\langle \varepsilon \rangle$ (or the spread in the values for different runs), the difference between the spatial and angular distributions of the L and R beams, and the error in the values of $\langle P(45°) \rangle$, was less than 0.01.

The intensity of the beam was continually monitored by a telescope comprising the three scintillation counters C_4-C_6, which registered protons scattered through $30°$ in the vertical plane by the polyethelene target. The position of this telescope was adjusted to give the maximum count rate each time the energy of the incident beam was changed in order to compensate for bending of the beam in the field of the polarized-target magnet. Scattering the particles in the vertical plane ensured that the monitor would be insensitive to changes in the beam polarization. The beam intensity was also measured at the energies 690, 760, and 804 MeV by counting coincidences from the counters C_1-C_3. The total count rate from the l and r channels of the polarimeter, which did not depend on the direction of the beam polarization, served as an additional monitor of the polarized-beam intensity. That the three monitors were all equally good is indicated by the fact that after the intensities (6) were determined and C_{NN} and P were calculated, the results obtained using the different monitors agreed with one another within the statistical error of the measurements. By directly counting the number of particles at low energies and measuring the intensity of the pp scattering by the polarimeter, we were able to estimate the absolute intensity of the polarized beams with an error of some 10–20%. The measured intensities and polarizations of the beams in the 690–950 MeV range are presented in Table II, together with the values used to estimate $\langle P(45°) \rangle$.

The polarized proton target[14] consisted of small spheres of propanediol ($C_3H_8O_2$) containing some $K_2Cr_2O_7$, held in a thin-walled resonator 13.7 cm^3 in volume. The polarization of the protons in the target was measured within 3% by the NMR signal and amounted to 85–95%. To test the accuracy in determining the polarization of the proton target we measured the asymmetry in the scattering of 610-MeV unpolarized protons by the polarized target. The target polarization found in this way agreed within the measurement errors (4%) with the result of the NMR measurement. The temperature of the polarized target was 0.04 –0.06 °K. At that temperature the relaxation time of a specimen target was about 1000 hr. The target was in the field (2.6 T) of a pair of superconducting Helmholtz coils 40 cm in diameter with a 30-mm gap between them. The entrance window of the target cryostat was covered with stainless steel foil 100 μm thick, and the exit window was covered with a mylar sheet 200 μm thick.

The working specimens were weighed after the experiment; their masses were in the range 9.0–10.3 g. We used a special 8.857-g graphite target to measure the background. The background target was held in a container identical to that for the working target and was mounted in place of the working target. The use of graphite prevented absorption of atmospheric water by

the background target.

The measurements were made with an apparatus that singled out correlated two-particle events. The scintillation counters $C_{15}-C_{22}$ (Fig. 1, a) were divided into two channels that registered registered pp events at c.m. angles of 90° and 50°. The angle of one of the telescopes of each channel was set at a value that was calculated after determining the angle through which the beam was bent by the magnetic field of the polarized target. The angle of the second telescope was set by verifying the linking of pp coincidences. The measuring apparatus was assembled in a standard CAMAC crate.

2. Separating the effect from the background. Results of the measurements

The data from the monitors, the polarimeter, and the recording channels were processed on line by a computer. The total statistics accumulated for each energy amounted to more than 4×10^4 events. To reduce the systematic error, the direction of the beam polarization was changed after 5×10^3 events had been accumulated or, in long runs, every two hours.

The background from parts of the apparatus and the nuclear component of the target was determined from measurements with the background target under identical kinematic conditions. In addition, the background of coincidences from parts of the apparatus alone was measured separately for each energy and polarization of the beam. As a result of the background measurements we introduced corrections to the actual weight of the working target and to the $^3\mathrm{He}-{}^4\mathrm{He}$ solution that filled the space between the propanediol spheres. The corrections amounted to 3–4%, depending on the experimental conditions.

The oxygen in the propanediol scatters nucleons less effectively than the carbon, so the count rate from the background target may be some 3% higher than the actual background. On the other hand, pions are produced on the protons in the propanediol, and that should tend to increase the actual background. As experiments with pure hydrogen at 970 MeV have shown,[15] the contribution from pion production under the pp elastic scattering peak varies, under otherwise identical conditions, from 1% at the c.m. angle 40° to 3% at 90°. As the energy decreases the contribution from inelastic processes decreases more rapidly than does that from pp elastic scattering. Thus, the background effects tend to cancel each other, and the measured intensities I_{+b} and I_{-b}, with allowance for a small correction to the actual weight of the specimen, correspond to the actual contribution from the nuclear component of the working target. Enough measurements with the background target were made to ensure that the error in determining the background would have little effect on the accuracy of the measurements of the desired quantities C_{NN} and P.

In order to verify that the procedure for measuring and allowing for the background at 950 and 690 MeV is correct, we measured the angular dependences of associated pp coincidences for the background target and
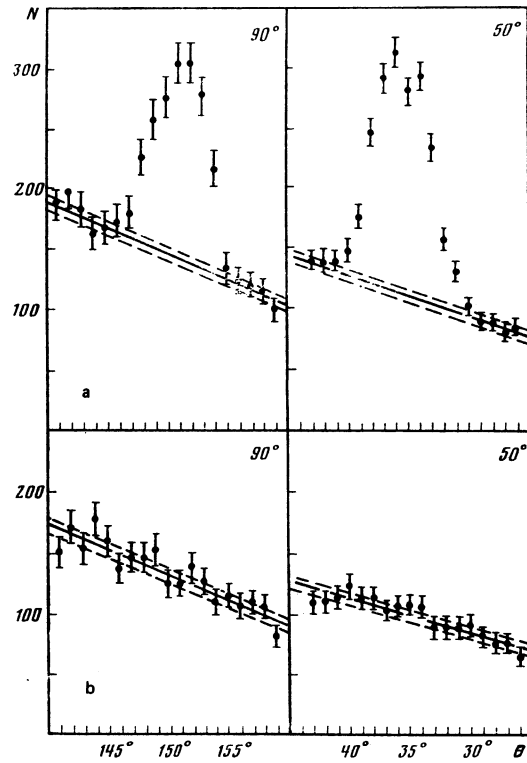

FIG. 2. Angular distributions of pp coincidences for the working (a) and background (b) targets at $T_p = 950$ MeV and $\theta = 50°$ and $\theta = 90°$ in the c.m.s. The abscissae are angles in the lab system, the position of $\theta_{lab} = 0$ being arbitrary.
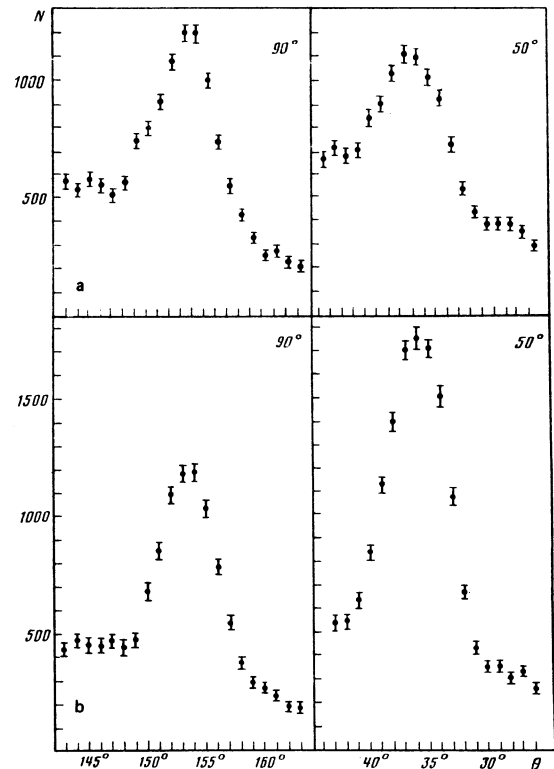

FIG. 3. Curves of correlated coincidences at $T_p = 690$ MeV: $a-P_B = 0$, $P_T = 0.9$; $b-P_B = 0$, $P_T = 0$. The abscissae are analogous to those of Fig. 2.

TABLE III. Values of the polarization correlation coefficient C_{NN} and the polarization in pp elastic scattering. *

550 MeV		610 MeV			630 MeV	
θ	C_{NN}	θ	C_{NN}	P	θ	C_{NN}
41°	0.54±0.05	40°	0.60±0.05	0.481±0.028	40.6°	0.44±0.05
69°	0.58±0.04	67°	0.57±0.04	0.326±0.010	69.6°	0.54±0.04
77°	0.53±0.04	78°	0.57±0.04	0.227±0.009	78°	0.60±0.04
91°	0.51±0.04	90°	0.57±0.04	−0.003±0.006	91°	0.66±0.04

T, MeV	NN (50°)	P(50°)	⟨P(50°)⟩	C_{NN} (90°)	P(90°)
690	0.540±0.030	0.525±0.014	0.516±0.009	0.740±0.030	−0.020±0.007
760	0.520±0.030	0.475±0.016	0.493±0.008	0.660±0.040	−0.049±0.007
804	0.558±0.025	0.484±0.014	0.468±0.008	0.589±0.033	0.011±0.010
840	0.560±0.040	0.458±0.014	0.449±0.008	0.670±0.060	0.062±0.011
892	0.550±0.030	0.430±0.011	0.423±0.009	0.610±0.040	−0.002±0.007
950	0.559±0.021	0.406±0.011	0.407±0.010	0.554±0.025	0.019±0.012

*The measurements at 550, 610, and 630 MeV were made at the JINR synchrocyclotron.[8]

the working target. Figure 2 shows the results of these measurements at 90° and 50° for the 950-MeV proton beam. The lines drawn along the "wings" of the angular dependence of the associated coincidences for the working target (Fig. 2, a) agree in slope and magnitude with the results obtained for the background target (Fig. 2, b). The measurements of associated coincidences at 650 MeV were carried through with polarized and unpolarized proton beam. Figure 3 shows the results of measurements of associated coincidences at 690 MeV for an unpolarized beam at angles of 90° and 50°. The difference between the intensities of pp coincidences for the polarized and unpolarized targets at 50° correspond well to the quantity $I_0 - I_0[1 - P_T P(50°)]$ (see the caption to Fig. 3). There is no difference beyond the statistical errors between the intensities at 90°.

The results of the measurements were processed with formulas (6)–(8). The values of C_{NN} and P are given in Table III. The errors include the errors in measuring the beam and target polarizations and the statistical error of the measurements. Calculating the polarization with Eqs. (8) and (9) yielded the same values.
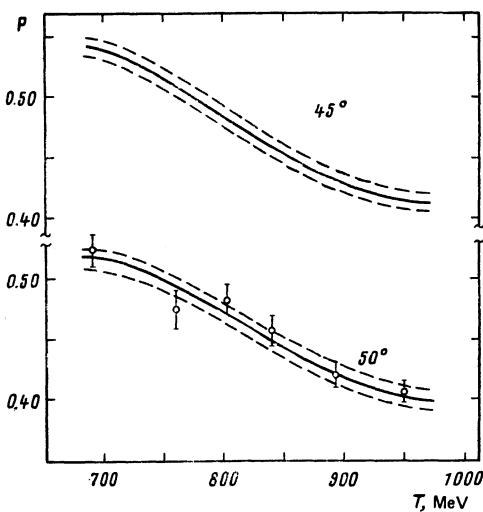
The fluctuations of $P(90°)$ about zero indicate that the choice of the working point by associated coincidences was accurate. The values of ⟨P(50°)⟩ given in the last column of the table were obtained by the same procedure as were the values of ⟨P(45°)⟩ (see above). Figure 4 shows the energy dependence of ⟨P(50°)⟩ obtained by averaging previously known data and the results of the present measurements. The same figure shows the energy dependence of ⟨P(45°)⟩ that was used to determine the polarizations of the beams.

III. DISCUSSION

The data on the coefficients C_{NN} and C_{LL} as functions of the incident-proton momentum for scattering at the c.m. angle $\theta = 90°$ are plotted in Fig. 5. The maximum at 700 MeV ($p \approx 1.3$ GeV/c), corresponding to predominance of the triplet interaction in the two-proton system, is prominent. It is difficult to estimate the relative magnitude of the contributions from the triplet and singlet interactions to the peak because of the large spread of the data at that energy; the ratio of the contributions is $(d\sigma_t/d\Omega)/(d\sigma_s/d\Omega) \approx 4$–10. The measurements of C_{NN}, C_{LL}, and the differential cross sections
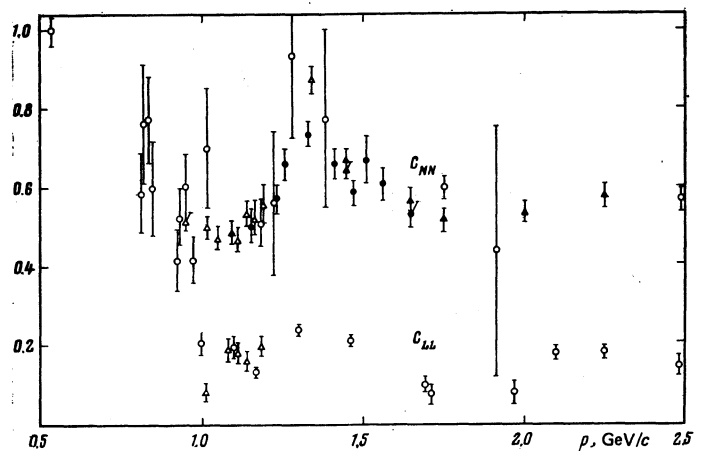

FIG. 4. Polarization in pp elastic scattering. The full curves are approximations to the data of Ref. 13 for $\theta_{c.m.} = 45°$ and 50°; the dashed curves mark the error corridors for the approximations; and the points represent the data of the present work.

FIG. 5. The polarization correlation coefficients C_{NN} and C_{LL} in pp scattering at $\theta_{c.m.} = 90°$ vs the incident-proton momentum. Points: O—Ref. 13, △—Ref. 10, ▲—Ref. 11, ●—Ref. 8 and the present work. Erratum: the uppermost open triangle should be a black triangle.
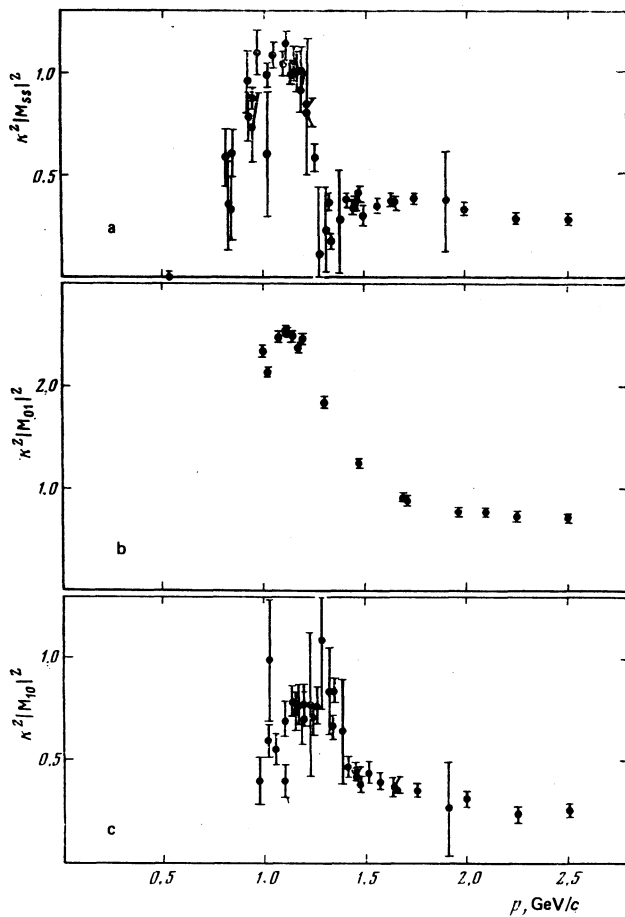
FIG. 6. The matrix elements M_{ss}, M_{10} and M_{01} for pp elastic scattering at 90° vs the incident-proton momentum p for $0.5 \leq p \leq 2.5$ GeV/c. The points represent experimental data from Refs. 8–11 and 13, and from the present work. Erratum: the numbers on the vertical scale of plot a should be doubled.

for scattering at $\theta = 90°$ make it possible to separate the contributions from individual matrix elements to the scattering at that angle. In addition to Eq. (2) for the matrix element M_{ss}, one can obtain

$$\frac{d\sigma_0}{d\Omega}(1+C_{LL})_{\theta=90°}=|M_{01}|^2,$$

$$\frac{d\sigma_0}{d\Omega}(C_{NN}-C_{LL})_{\theta=90°}=|M_{10}|^2. \qquad (12)$$

The first of these matrix elements, M_{01}, contains contributions from all the triplet states except the $^3P_0$ state, while the second of these matrix elements, M_{10}, contains contributions only from states with $J=L\pm1$, i.e. it does not depend on the $^3P_1$ and $^3F_3$ states. The momentum dependences of M_{ss}, M_{01}, and M_{10} are shown in Fig. 6, a, b, and c. The maximum in the singlet pp interaction is prominent; it is usually associated with the $^1D_2$ state (production of $N\Delta$ in the S state).[16] The dependence of the triplet matrix elements on the incident-particle momentum (Fig. 6, b and c) reveal very similar maxima at $p \approx 1.2$–1.3 GeV/c. This does not permit one to conclude that there is any considerable resonance contribution from the $^3P_0$ or $^3P_1$ states, which enter separately in the matrix elements. The same can be said for the resonance in the $^3F_3$ state, too, for that resonance does not manifest itself clearly enough
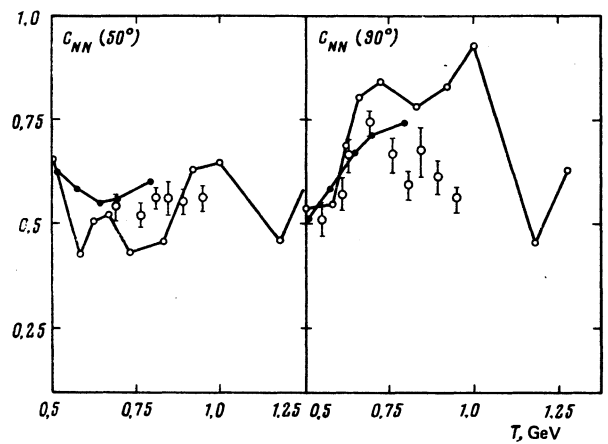

FIG. 7. Comparison of the experimental results of the present work and Ref. 8 (large open circles) with the predictions of the phase-shift analyses of Ref. 4 (small open circles) and Ref. 17 (black circles).

either.

The results of the present work were compared with the phase-shift analyses of Refs. 4 and 17, which are not inconsistent with the hypothesis of dibaryon resonances. The comparison (Fig. 7) showed serious discrepancies between the predictions of the phase-shift analysis of Ref. 4 and the experimental data in the region $\theta = 90°$, $T \geqslant 800$ MeV. The phase-shift analysis of Ref. 17 is limited to the energy 800 MeV and is in satisfactory agreement with our experimental data. The energy dependence of $C_{NN}(50°)$ reveals no noticeable features and is not in conflict with the predictions of the phase-shift analyses. Thus, the data under consideration do not provide grounds for drawing any definite conclusions concerning the resonance character of the interaction in the two-proton system in the investigated energy range. The structure observed in the energy dependence of $C_{NN}(90°)$ is a consequence of the difference between the energy dependences of the singlet and triplet pp-scattering amplitudes. One of the reasons for this effect, aside from the hypothesized resonance states of two protons, might be a contribution from inelastic processes to the singlet $^1D_2$ state in the 550–750-MeV energy region, as was qualitatively shown by the example of the difference between the total cross sections for pp interaction in the singlet and triplet states.[18,19]

[1]I. P. Auer, E. Colton, D. Hill, et al., Phys. Lett. 67B, 113 (1977); Phys. Lett. 70B, 475 (1977); Phys. Rev. Lett. 41, 354 (1978).

[2]W. de Boer, R. C. Fernov, A. D. Krisch, et al., Phys. Rev. Lett. 34, 558 (1975). Ed. K. Biegert, J. A. Buchanan, J. M. Clement, et al., Phys. Lett. 73B, 235 (1978).

[3]H. Hidaka, A. Beretwas, K. Nield, et al., Phys. Lett. 70B, 479 (1977).

[4]Norio Hoshizaki, Progr. Theor. Phys. 60, 1796 (1978); 61, 129 (1979).

[5]Akihiko Yokosawa, Phys. Rep. 64, 47 (1980).

[6]Malcolm H. Mac Gregor, Phys. Rev. D20, 1616 (1979).

[7]P. J. G. Mulders, A. Th. M. Aerts, and J. J. de Swart, Phys. Rev. Lett. 40, 1543 (1978); Phys. Rev. D17, 260

(1978).

[8]N. S. Borisov, L. N. Glonti, M. Yu. Kazarinov, *et al.*, Zh. Eksp. Teor. Fiz. **72**, 405 (1977) [Sov. Phys. JETP **45**, 212 (1977)].

[9]H. E. Dost, J. F. Arens, F. W. Betz, *et al.*, Phys. Rev. **153**, 1394 (1967). G. Cozzika, Y. Ducros, A. de Lesquen, *et al.*, Phys. Rev. **164**, 1672 (1967).

[10]D. Besset, Q. H. Do, B. Favier, *et al.*, Phys. Lett. **94B**, 310 (1980). M. W. McNaughton, H. W. Baer, P. R. Bevington, *et al.*, Phys. Rev. **C23**, 838 (1981).

[12]V. G. Vovchenko, A. A. Zhdanov, V. M. Zheleznyakov *et al.*, Preprint LIYaF-576, 1980.

[13]J. Bystricky and F. Lehar, NN-scattering data, Karlsruhe, 1978.

[14]N. S. Borisov, E. I. Bunyatova, Yu. F. Kiselev *et al.*, Preprint JINR-13-10253, 1976.

[15]V. G. Vovchenko, A. A. Zhdanov, V. M. Zheleznyakov *et al.*, Preprint LIYaF-212, 1976.

[16]R. Ya. Zul'karneev and A. M. Rozanova, Preprint JINR R2-5058, 1970.

[17]R. Arndt and B. J. Verwest, NN-scattering analysis below 850 MeV. Status report, 1980.

[18]C. L. Hollas, Phys. Rev. Lett. **44**, 1186 (1980).

[19]W. M. Kloet, J. A. Tjon, and R. Silbar, Phys. Lett. **99B**, 80 (1981).

Translated by E. Brunner